California Solar Initiative

RD&D: Research, Development, Demonstration and Deployment Program

GO solar CALIFORNIA

Final Project Report:

Forecasting and Storage Control to Mitigate Large Ramps

Grantee:

University of California San Diego

July 2016

www.CalSolarResearch.ca.gov

PREPARED BY

UC San Diego
JACOBS SCHOOL OF ENGINEERING

9500 Gilman Drive
La Jolla, CA 92093-0411

Principal Investigator:
Jan Kleissl
jkleissl @ ucsd.edu
858-534-8087

Dept of Mechanical & Aerospace EngineeringCenter for Renewable Resources &Integration and the Center for Energy Research

Project Partners:
San Diego Gas & Electric

PREPARED FOR

California Public Utilities Commission
California Solar Initiative: Research, Development, Demonstration, and Deployment Program

CSI RD&D PROGRAM MANAGER

Itron CSI RD&D Program Manager

Program Manager:
Smita Gupta
Smita.Gupta @ itron.com

Project Manager:
Stephan Barsun
Stephan.Barsun @ itron.com

Additional information and links to project related documents can be found at
http://www.calsolarresearch.ca.gov/Funded-Projects/

Preface

The goal of the California Solar Initiative (CSI) Research, Development, Demonstration, and Deployment (RD&D) Program is to foster a sustainable and self-supporting customer-sited solar market. To achieve this, the California Legislature authorized the California Public Utilities Commission (CPUC) to allocate **$50 million** of the CSI budget to an RD&D program. Strategically, the RD&D program seeks to leverage cost-sharing funds from other state, federal and private research entities, and targets activities across these four stages:

- Grid integration, storage, and metering: 50-65%
- Production technologies: 10-25%
- Business development and deployment: 10-20%
- Integration of energy efficiency, demand response, and storage with photovoltaics (PV)

There are seven key principles that guide the CSI RD&D Program:

1. **Improve the economics of solar technologies** by reducing technology costs and increasing system performance;
2. **Focus on issues that directly benefit California**, and that may not be funded by others;
3. **Fill knowledge gaps** to enable successful, wide-scale deployment of solar distributed generation technologies;
4. **Overcome significant barriers** to technology adoption;
5. **Take advantage of California's wealth of data** from past, current, and future installations to fulfill the above;
6. **Provide bridge funding** to help promising solar technologies transition from a pre-commercial state to full commercial viability; and
7. **Support efforts to address the integration of distributed solar power into the grid** in order to maximize its value to California ratepayers.

For more information about the CSI RD&D Program, please visit the program web site at www.calsolarresearch.ca.gov.

Abstract

An optimization routine was formulated that uses solar forecasting to control battery energy storage and a PV inverter to mitigate ramp rates in PV power output. The efficacy of ramp rate control was evaluated for a summer and winter period using real irradiance data and real sky imager solar forecasts. A cloud base height algorithm was developed to improve solar forecast accuracy. For the majority of battery configurations, the use of sky imager forecasts reduces ramp violations compared to the same method without forecasting, but requires greater battery energy dispatch and energy curtailment via the inverter.

1. Background

The California Public Utilities Commission (CPUC) required acquisition of energy storage resources by the investor-owned utilities (IOUs) in the state. A primary application of energy storage is mitigating fluctuations in net load (or the variability in net load from forecast net load), aiding the integration of intermittent renewable energy resources. Especially in small geographic areas such as those served by a distribution feeder or microgrid, solar generation is the primary contributor to net load variability. Unfortunately, the high cost of energy storage may limit the penetration of solar capacity on feeders to 15% even as the cost of solar generation has plummeted. Enabling the CPUC goal of reducing energy storage costs, this research project investigated whether storage controls for ramp mitigation will reduce the quantity of storage needed while achieving the same benefits as an uncontrolled energy storage system.

Increasing solar PV penetration on distribution feeders eventually causes sharp ramping of feeder net load and results in voltage fluctuations beyond acceptable limits. Utility scale energy storage at the substation can counteract these ramps. However, lacking advance knowledge of solar energy production, the state of charge for a battery system is not optimized to mitigate incipient solar ramps. Coupling solar forecasting for power prediction to a feed-forward battery controller, the battery state of charge can be adjusted in advance of sharp changes in solar energy production. Thus limited and costly battery capacity will be used more intelligently and efficiently, reducing the size of battery required as well as reducing frequency of deep discharges, thereby extending battery life and reducing system life cycle costs. This final report summarizes overall project accomplishments. More details can be found in the two task reports.[1]

2. Importance of Cloud Base Height for Short-term Solar Forecasting

Short-term solar forecasting has become an important need in the solar industry. Cloud base height (CBH) is a major source of forecast error during short-term solar forecasting. Incorrect CBH leads to an offset between the vertical projection of a cloud onto the ground and the actual shadow location. In addition, inaccurate cloud speed associated with CBH errors causes errors in the estimates of arrival time of cloud shadows, which leads to offsets in ramp timing.

Numerical weather prediction and satellite forecasting of solar radiation in the 0 – 20 minute-ahead time frame poses challenges due to limited resolution and long response time. Sky-imaging observations are advantageous because one instrument can accurately determine the current distribution of cloud cover at high spatial and temporal resolution and - after obtaining cloud speed and optical depth - forecast power production within the 0 – 20 min time window. However, a limitation is the lack of absolute measurements of CBH, as single point imaging only obtains two-dimensional projections (Figure 1).

[1] http://www.calsolarresearch.org/funded-projects/118-mitigation-of-fast-solar-ramps-through-sky-imager-solar-forecasting-and-energy-storage-control

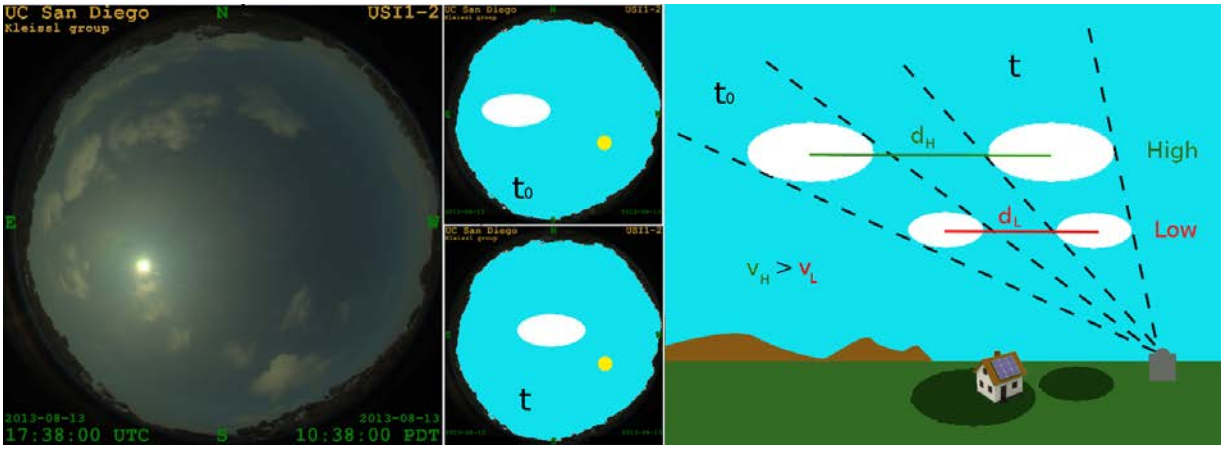

Figure 1 Left: Sample image taken with the UCSD Sky Imager (USI). Center: Two consecutive simulated images showing cloud motion from time t_0 to time t. Right: Schematic depiction of the effect of cloud height on cloud speed and shadow size and location at time t.

Clouds differing in size and height can yield the same representation in the image (right sketch). Therefore for accurate georeferencing, it is necessary to determine the absolute CBH. While ceilometers or stereographic method applied to additional sky imagers can be used to obtain CBH, they result in increased cost and complexity. The project team integrated an inexpensive cloud speed sensor (CSS) that was developed at UC San Diego into a sky imaging system to scale imaging data with absolute position data.

3. Measurement setup

The CSS is a compact and economical system that measures cloud shadow motion vectors. The system consists of an array of eight satellite phototransistors (TEPT4400, Vishay Intertechnology Inc., USA) positioned around a phototransistors located at the center of half circle of radius 0.297 m, covering 0-105° in 15° increments (Figure 2). A CSS, a UCSD sky imager (USI), and (for validation) a ceilometer were setup at the UC San Diego campus (Figure 3). The USI can be used to detect cloud fields and track cloud motion. These measurements yield forecast of future cloud locations at high spatial and temporal resolutions and improve forecast skill up to a 20 min forecast horizon. The benefit of using sky imager observations over a large ground sensor network is that only one or a few instruments deployed around the area of interest are capable of determining the current distribution of cloud cover at a high resolution.

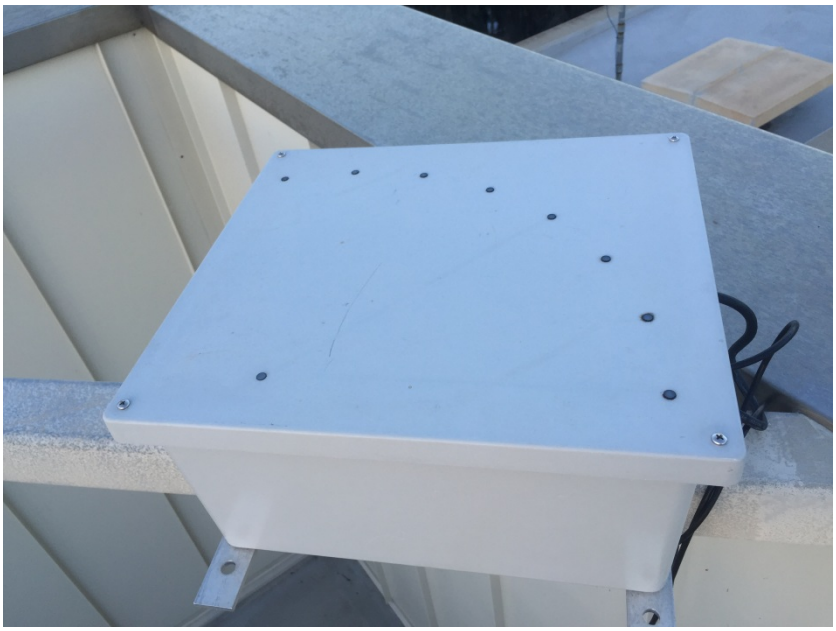

Figure 2 Cloud shadow Speed Sensor (CSS) contained inside a weather proof enclosure with dimensions 0.45 x 0.40 m. On the top of the enclosure is an array of nine phototransistors.

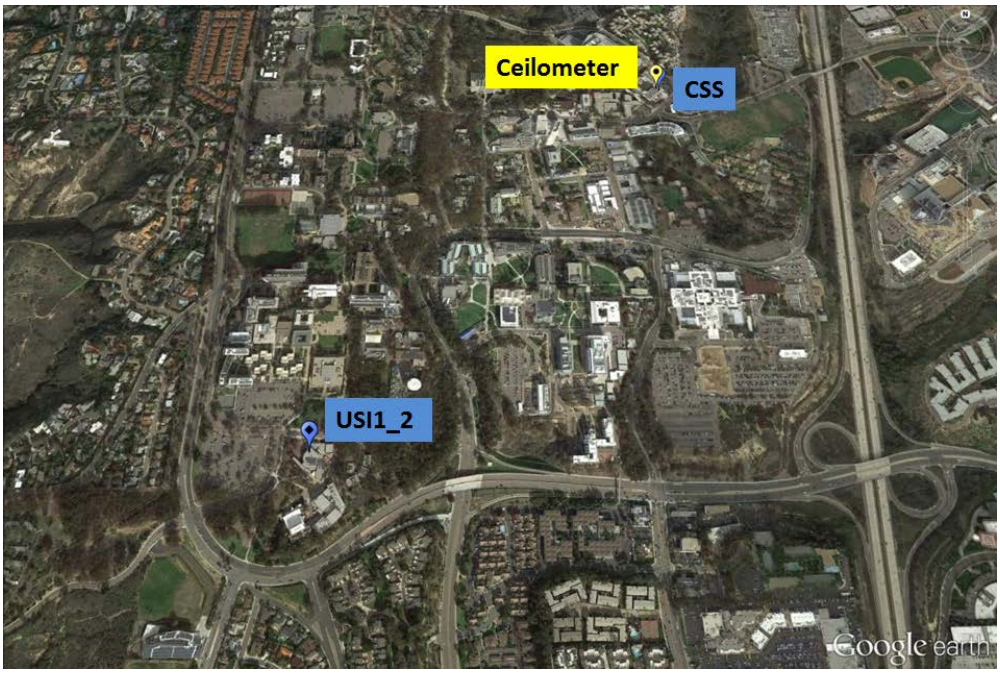

Figure 3: Locations of sky imager (USI1_2) and ceilometer and Cloud Shadow Speed Sensor (CSS) installations on the UCSD campus. The straight-line distance between USI and CSS is 1.25 km. Map data ©2015 Google.

Figure 4 shows a set of cloud speeds and directions for one day. Clouds move slowly at up to 6 m s^{-1} from north to south changing to easterly as the day progresses. There is some variability in the signal, but that is likely a result of both physical cloud dynamics and sensor noise. A wind-rose plot shows the histogram of the motion vectors on this day by showing the frequency of speed

and direction pairs. It is noticeable that most motion vectors cluster in north-east direction with an average speed range of 2-6 m s^{-1}.

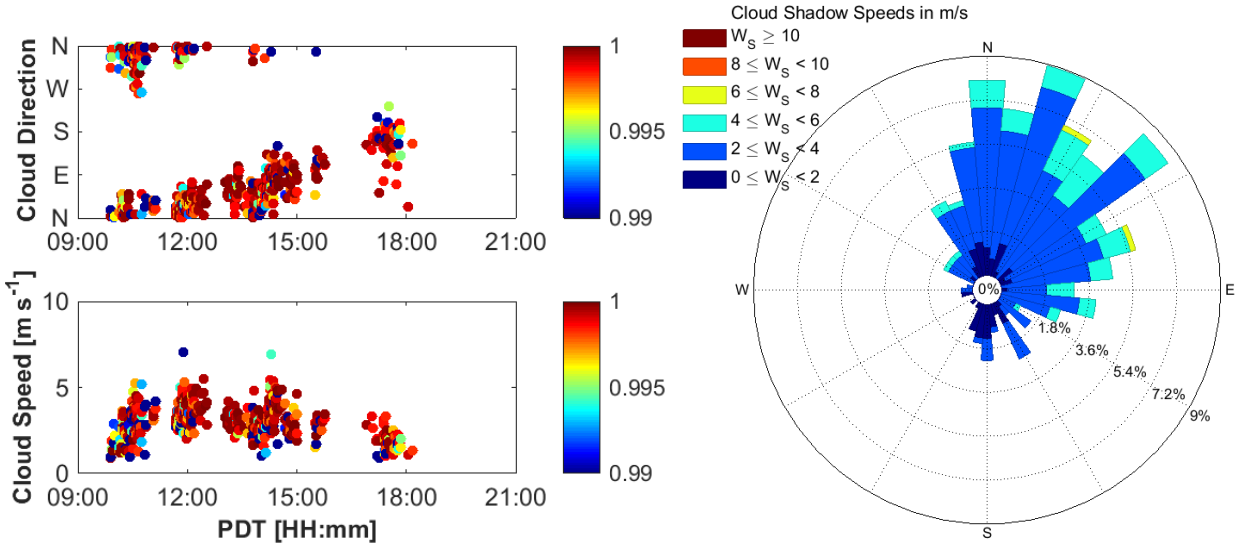

Figure 4: Cloud direction and cloud speed determined by the curve fitting method on May 31th, 2015 using 9 sec segments of CSS data. The color provides the average cross correlations R_{ij} for each pair of points during each 9 sec cycle. Right: Wind-rose plot of cloud direction and cloud speed shown on the left. The color bins show cloud speed range, and the values on concentric circles represent the frequency of appearance of each cloud speed bin.

4. Cloud base height algorithm

With independent measurements of cloud speed from the CSS, U_{CSS}, the local CBH (labeled as $CBH_{CSS+USI}$) can be obtained as

$$CBH_{CSS+USI} = \frac{U_{CSS} \times n}{U_{pixel} \times 2tan\theta_m}.$$

U_{USI} is cloud speed in units of m s^{-1} determined by USI, U_{pixel} is image-average cloud pixel speed in units of pixel s^{-1} obtained through the cross-correlation method applied to two consecutive USI images, θ_m is the maximum field of view of the USI (here $\theta_m = 80^\circ$), $CBH \times 2tan\theta_m$ is the horizontal length of the sky imager view domain (termed "cloud map"), and n is the number of pixels in the cloud map.

With all other parameter as constants, CBH depends on the ratio of U_{CSS} and U_{USI}. The algorithm is implemented into the USI forecast algorithm to calculate local CBH at each step using the most recent CSS measurement.

5. Cloud base height validation

5.1 CBH validation examples for one sample day

A detailed example is analyzed in this section. Figure 5 shows the CBH comparison among ceilometer measurements and the CBH method based on CSS and USI for one day with different cloud types and multiple cloud layers, ideal to ascertain the robustness of the method. On this day, the period from 16:00 to 17:30 UTC is characterized by nearly overcast stratus clouds that turn into few alto-cumulus at the same altitude. During 18:30-21:45 UTC, scattered cumulus dominate, while after 21:45 UTC, broken cumulus are observed. UTC lags local daylight savings time (PDT) by 7 hours.

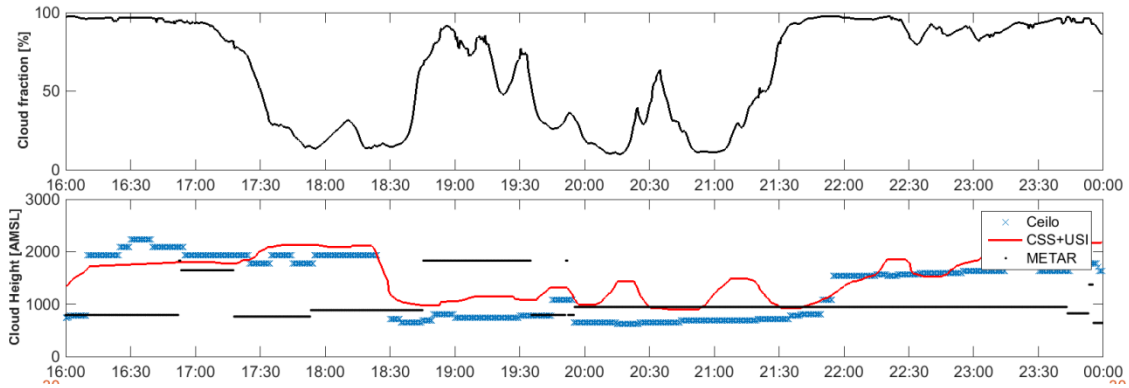

Figure 5: Sample comparison among different CBH measurements on May 22, 2015. The x axis is time in Universal Coordinated Time (UTC). Top: Cloud fraction in units of % during the day. Middle: CBH comparison between local ceilometer measurements (blue crosses), and the proposed method combining USI and CSS cloud speed measurements (red line). See Figure 3 for locations of the instruments. The black dots indicate the CBH measurement from a ceilometer at Miramar Naval Air Station (KNKX), 8.8 km to the east.

In the middle plot of Figure 5, both local ceilometer measurements (the ground truth) and optimized CBH yield the same trend. For example, between 16:00-18:30 UTC, the present method produces similar CBHs as the local ceilometer at about 2,000 m, while the airport ceilometer reports 800 m. At 18:30 UTC, ceilometer measurements indicate a CBH transition from about 2,000 m to 750 m, and the CBH from CSS & USI follows this transition, although with about a 300 m offset. After 21:00 UTC, an additional cloud layer with different direction/speed at times temporarily confuses the $\mathrm{CBH}_{\mathrm{CSS+USI}}$, as evident in brief elevated CBH around 21:15 UTC and 22:15 UTC. However, the curve fitting method still captures the CBH transition detected by the ceilometer from 800 m to 1,500 m at 22:00 UTC, and follows the ceilometer measurement until the end of the day. In summary, the proposed method is accurate on this day especially in the morning. The daily RMSD is 343 m and nRMSD is 23.2%.

5.2 CBH validation statistics

Over all 16 validation days, average root mean square difference (RMSD) values were below 160 m and 17.4% on all 16 days, while the nRMSD remains below 28%. The daily biases are usually less than 80 m and the overall bias is only 2 m indicating that most of the RMSD is driven by shorter-term random fluctuations that are difficult to model. Most days have low cumulus and stratus clouds, and the CBH results generally agree with the RMSD as low as 30 m and 7.5% for nRMSD. On the other hand, CBH from the nearest airport delivers CBH with large offset to local

CBH and ceilometer, which further demonstrates the spatial variability in cloud coverage and height. The proposed method is therefore expected to be superior for short term solar forecasting.

6. Solar Forecasts for Ramp Rate Control of Energy Storage

Several technologies are available to mitigate ramp rates from PV systems. A battery energy storage system (BESS) co-located with a PV power plant can attenuate ramps by charging and discharging at opportune times. Inverter control offers an additional measure of mitigation via energy curtailment during up-ramps. Sufficiently accurate forecasts are expected to facilitate such mitigation with fewer charge cycles and less energy curtailment. Together, BESS and inverter control with short-term solar forecasts provides a solution for operators of PV systems who wish to mitigate excessive ramp rates in PV power output.

A ramp rate control algorithm was developed to control a BESS and inverter to mitigate ramps in PV power output greater than 10% per minute using sky image-based solar forecasting. Numerous simulations were run to understand the implication of key model parameters, including BESS sizing and forecast accuracy. While the original proposal envisioned a hardware demonstration, attempts to commission an existing BESS were unsuccessful due to issues with the battery control and communications systems, which are described in detail in the Appendix of the task report. Therefore, this report presents only simulation results.

7. Ramp rate control algorithm

7.1. Concept

Figure 7 depicts the operation of the control algorithm. For a forecasted down-ramp—that is, for clear sky conditions and an approaching cloud—the BESS charges prior to the start of the ramp and during the ramp. Conversely, for a forecasted up-ramp—that is, for cloud shadows leaving the footprint of the PV system—an optimal amount of PV power output charges the BESS, and less power therefore reaches the medium voltage grid. If the BESS reaches its rated charge, the inverter may reduce throughput. With either BESS or inverter control during up-ramps, the system achieves the same result—less power reaches the grid. In this way, the system mitigates the forecasted up-ramp and prevents exceedances of the ramp rate threshold.

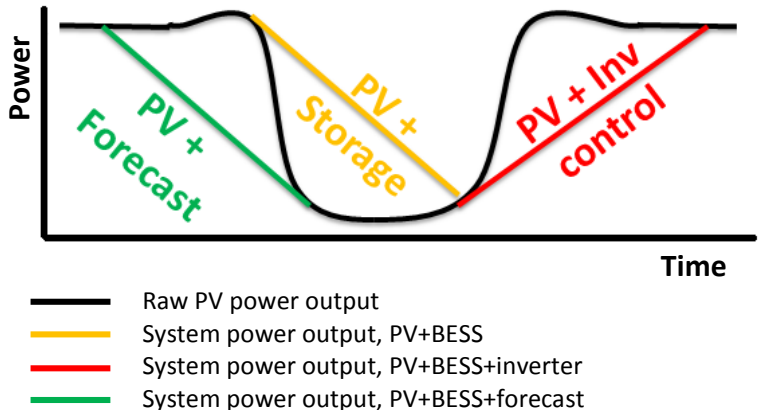

Figure 6 – A conceptual schematic shows the operation of the control algorithm. The "system" consists of a PV array, BESS, inverter, and solar forecasting. Without BESS and inverter control, ramp violations are frequent (black). The addition of a BESS and inverter provides reactive ramp smoothing (yellow, red). The further addition of forecasting provides proactive ramp smoothing (green); the response is proactive because the BESS charges prior to the ramp violation.

7.2. Control Algorithm

The control algorithm is formulated as a discrete-time, linear optimization problem. At each time step the control algorithm seeks to maximize power output from the PV system, and also to maintain the BESS at the idle, or preferred, state-of-charge (SOC)—0.5 in the simulations. In the cost function these two considerations compete with one another, and thus weights are used to assign relative importance.

Constraints maintain system dynamics—for example, by preventing the BESS from exceeding its rated capacity—and impose thresholds on the system ramp rate. Bounds ensure the inverter and BESS are not controlled beyond their limits. The inverter permits throughput between 0 and 100% of potential PV power, the former being full curtailment and the latter full throughput.

As penalties for ramp rate violations and explicit markets for battery storage have not yet been codified, and as revenue for solar PV generation varies, the optimization routine is written with the absolute edict "to not have ramp violations". As regulations, penalties, and markets emerge, this work could be developed further to include the monetization of ramp violations, PV power production, and BESS cycling.

The control algorithm is parameterized using system specifications and the threshold for ramp rate violations. A comprehensive list of model parameterizations is presented in Table 1.

Table 1 – Control algorithm parameterizations

Parameter type	Parameter	Units
PV system	Rated AC capacity	kW
BESS	Maximum capacity	kWh
	Minimum capacity	kWh
	Maximum discharge capacity	kW
	Maximum charge capacity	kW
	Discharge efficiency	-
	Charge efficiency	-
	Idle state-of-charge	-
Inverter	Minimum allowable throughput	-
Forecast	Forecast horizon	minutes
Ramp rate	Ramp rate threshold	% $p_{PVkWac,peak}$ min^{-1}

7.3 Input and output

Once parameterized (with those parameters in Table 1), the control algorithm requires only forecasted PV power output to the specified forecast horizon and measured PV power output from the previous two timesteps. Measured power output is required to calculate the current ramp rate of the PV system, whereas the forecasted power output provides a "schedule" of upcoming ramps, which the algorithm uses to determine optimal control of the BESS and inverter.

The output of the control algorithm is the optimal dispatch schedule for the BESS and control of the inverter that minimizes the cost function for the forecast horizon.

7.4 Selection of data and characterization of variability

To quantify the performance of the ramp rate control algorithm many different seasonal and cloud conditions were sought and motivated simulations for a summer period—30 days in June and July 2014—and a winter period, November 2014. In this final report only results for the summer period are shown.

In the context of ramp rate control, the PV power output alone can be thought of as "uncontrolled" power output. The subsequent control of a BESS and inverter, summed with the uncontrolled power, thus represents the "controlled" power output. Ramp rates and ramp violations in the uncontrolled power time series for the selected time periods are presented in Figure 8.

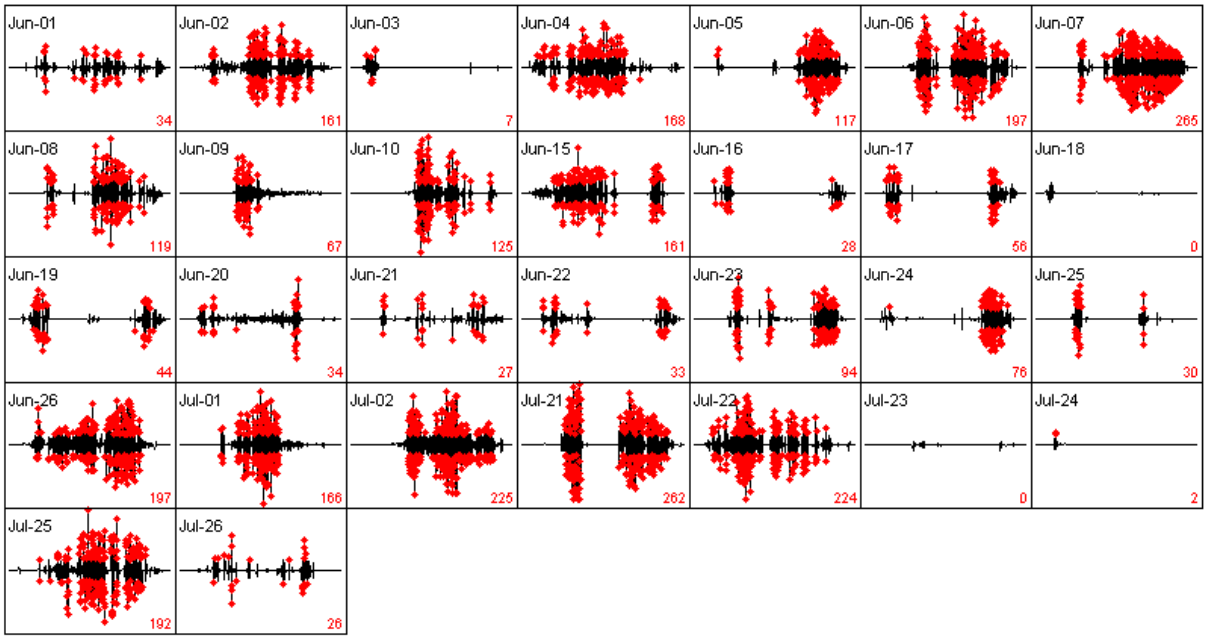

Figure 7 – Ramp rates and ramp violations in the PV power output measured at UC San Diego during selected days in June and July 2014. The number of daily ramp violations is presented at the bottom right. Ramp rates are shown as black line with black dots, but when the ramp rate exceeds 10% / min the dots are colored red.

8. Ramp Rate Control Simulations

8.1. Sample Day

Simulations were run for the summer and winter periods in two separate domains: first, to explore the relationship between BESS sizing and ramp violation mitigation; and second, to explore the efficacy of the sky imager forecasts to facilitate ramp violation mitigation by simulating ramp smoothing using also persistence forecasts and perfect forecasts. Persistence forecasts project measured PV power output at the current timestep through the entire forecast horizon. Using persistence forecasts is therefore equivalent to using no forecasts. Perfect forecasts, on the other hand, use back-casting (that is, future PV power output) in place of forecasts; at each timestep, the perfect "forecast" is therefore 100% accurate.

To illustrate the operation of the ramp rate control algorithm, the uncontrolled power output (that is, the raw PV power output without a BESS or inverter control) is plotted with the controlled or system power output. "System" means the sum of PV power output, BESS output, and inverter curtailment. The time series for power output and ramp rates for the PV array and system are presented in Figure 9 for November 15, 2014, the second cloudiest day in November 2014. Significant ramp amplitudes—greater than +/- 25% / min of the nameplate capacity of the PV system—are observed in the uncontrolled PV power output. Together, the control of the BESS and inverter mitigates the majority of ramp violations, though the largest down-ramp violations are not mitigated because the BESS kW capacity is too small. Significant inverter curtailment is required to mitigate the largest up-ramp violations.

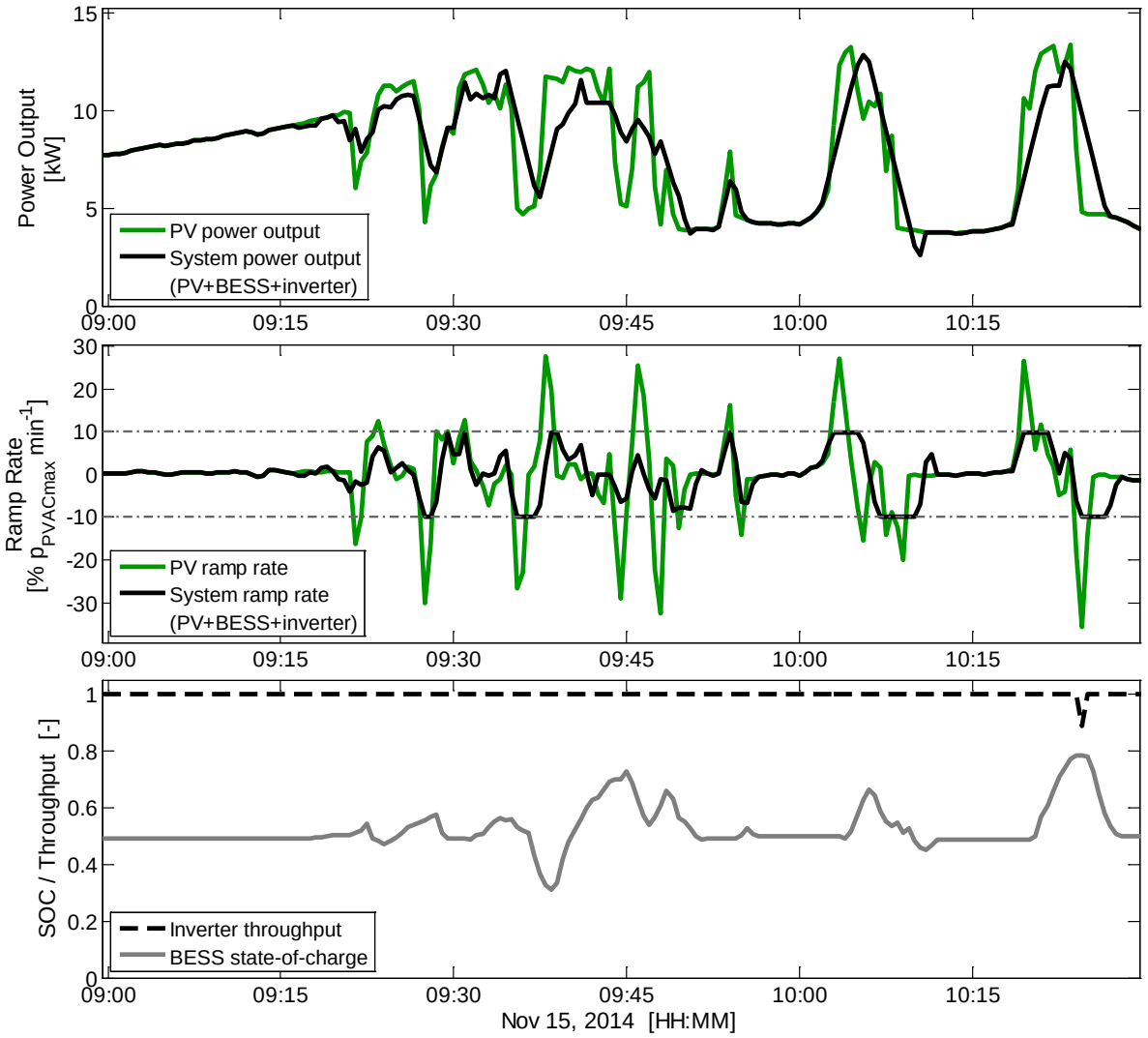

Figure 8 – The uncontrolled PV power output and system power output (top), ramp rates and the +/- 10 percent per minute ramp rate threshold (middle), and BESS dispatch and inverter throughput (bottom) for 09:00–10:15 on November 15, 2014 using sky imager forecasts. All ramp violations are mitigated. A 24 kWac PV array, a 5 kW / 0.5 kWh = 10 kW / kWh BESS, and sky imager forecasts were used.

8.2 Performance with respect to BESS sizing

To explore the relationship between BESS sizing and ramp violation mitigation, numerous BESS configurations were simulated—energy capacities from 0.083-1 kWh and dispatch capacities from 1-10 kW. The PV system has nameplate capacity 24 kWac, and thus the selection of configurations covers a wide range of capacities relative to the PV system. The BESS dispatch capacities (1 to 10 kW) range from 4–41% of the PV capacity, and the range of energy capacities (0.083 to 1 kWh) can, when fully charged, accommodate maximum discharge for approximately 0.5 to 60 min, a wide range—many of the energy-dispatch ratios are not proportional (that is, optimally selected) for ramp smoothing, but were included in the analysis to bookend the simulation results.

The results of ramp smoothing simulations for all BESS configurations and using sky imager forecasts are presented in Figure 10 for the summer period. A wide range of BESS dispatch and inverter curtailment achieves a similarly wide range of ramp violation mitigation. Improvement in ramp violation mitigation is achieved most precipitously when the BESS dispatch capacity is increased from 1 to 4 kW; further mitigation is achieved thereafter but at a lesser rate of improvement. Increase in the energy capacity results in a less marked improvement. The trends in ramp violation mitigation are presented in a different visualization—as data series of constant capacities—in Figure 11.

Significant inverter curtailment is used for the smallest BESS dispatch capacities (1-2 kW); consequently, less total BESS dispatch is used. The need for curtailment falls off quickly with increasing dispatch capacity; again, consequently, the total BESS dispatch needed increases quickly in response.

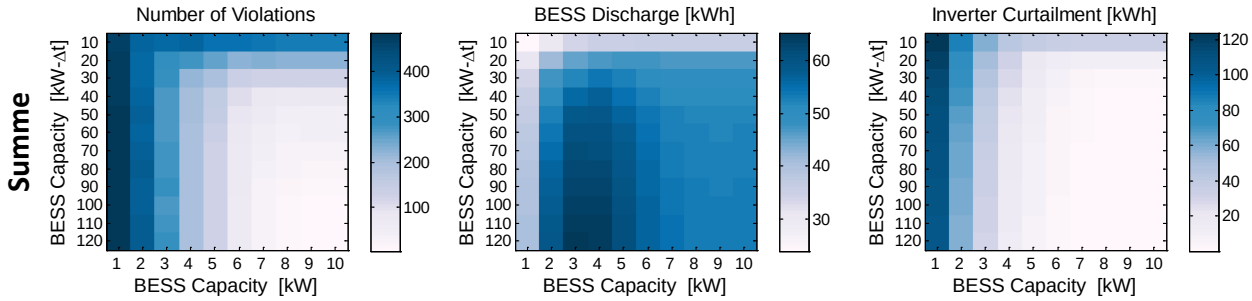

Figure 9 – The number of total ramp rate violations (left), total energy discharged from the BESS (middle), and total energy curtailed at the inverter (right) are shown for the range of BESS capacities simulated for the summer period. Sky imager forecasts are used. 120 kW Δt equals 1 kWh.

The number of total ramp rate violations in Figure 10 is plotted in Figure 11 as individual contours of constant dispatch (kW) and energy capacity. Figure 11 shows clearly that for certain BESS configurations—both constant dispatch capacity and constant energy capacity—a threshold is reached after which any increase in the other capacity does not bring about further mitigation. This trend is most salient with lines of constant dispatch capacity (kW).

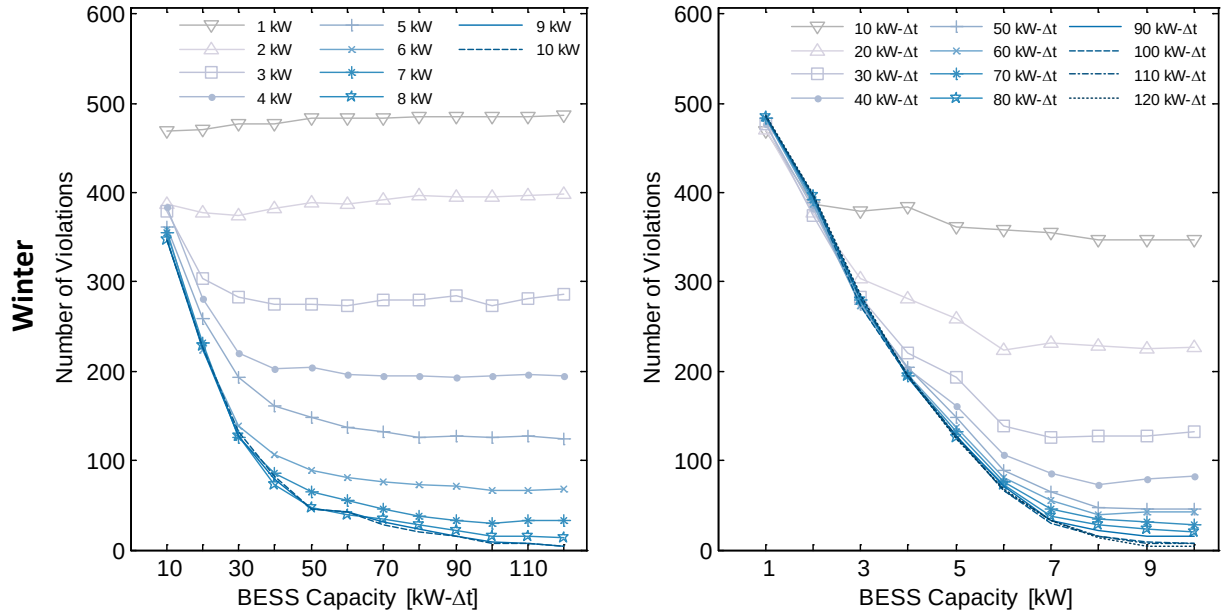

Figure 10 – The number of total ramp violations for individual contours of constant energy capacity (left) and constant dispatch capacity (right) for the summer period. Increasing the energy capacity for data series of constant dispatch capacity (left) improve ramp violation mitigation, but each dispatch capacity has a threshold after which ramp violation mitigation no longer improves with increasing energy capacity. The same is true, but less precipitous, for increasing dispatch capacity and constant energy capacity (right).

8.3 Performance with respect to forecasting

In this section the efficacy of the sky imager solar forecast to facilitate ramp violation mitigation is quantified. Simulations with sky imager solar forecasts as inputs to the ramp rate control algorithm were followed by identical simulations using, separately, persistence forecasts and perfect forecasts. The perfect forecast, though impracticable, provides an upper limit on ramp violation mitigation for a given BESS configuration. Comparing the efficacy of these three forecast methodologies—sky imager, persistence, and perfect forecasts—provides further insight into the utility of the sky imager forecast.

Figure 12 presents the difference in results between the sky imager and persistence forecasts. The difference is calculated as the results of the sky imager forecast minus those of the persistence forecast; positive values therefore denote a greater occurrence (for example, more violations) using sky imager forecasts. In both seasonal periods, the sky imager forecasts use greater BESS dispatch and inverter curtailment. The use of sky imager forecasts affects greater ramp violation mitigation in all cases except for smaller BESS dispatch capacities during the summer period (less than 5-6 kW). The summer period in coastal San Diego contains large and frequent ramp rates and thick stratocumulus clouds that form and dissipate typically daily, which are difficult to forecast. Smaller BESS capacities combined with inaccurate forecasts therefore challenge the ramp violation mitigation potential of the system. Larger BESS dispatch capacities have a greater capacity to compensate for sky imager forecast error and therefore outperform the persistence forecasts.

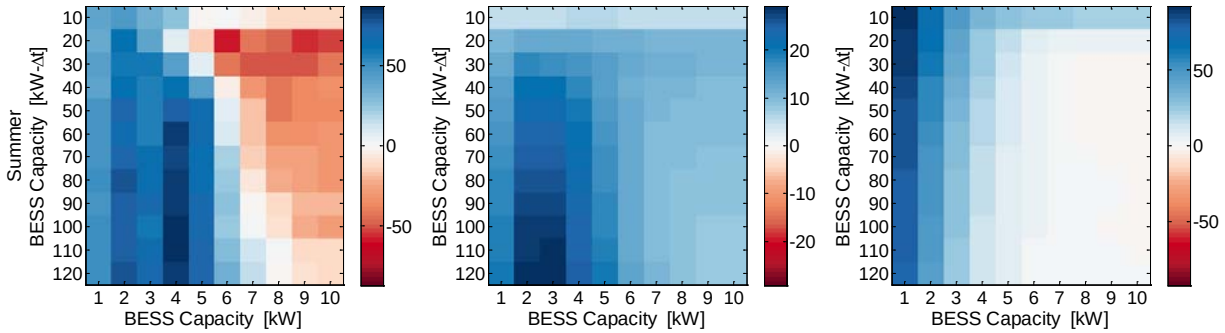

Figure 11 – The difference in total number of violations (left), difference in total BESS dispatch (middle) and difference in inverter curtailment (right) for the summer period. The difference calculated is the results of using the persistence forecast subtracted from the results of using the sky imager forecast—positive values therefore represent a greater occurrence when using the sky imager forecast.

Ramp rate control without forecasting is possible but is severely handicapped: though the BESS dispatches optimally during a ramp, without a prediction of upcoming ramps, it dispatches reactively, never proactively. Forecasts predict ramps prior to their occurrence, which allows the BESS to dispatch optimally prior to the ramp, as well as during it. Ramp rate control with accurate forecasting is therefore superior to control without it, in theory. In other words, solar forecasts allow a smaller BESS to achieve the same performance as a larger BESS without forecasting.

9. Discussion and Conclusions

In this report a sensor and an algorithm to provide an accurate local CBH for sky imager solar forecasting was introduced. CBH can then be derived by comparing CSS cloud speed measurements in [m s^{-1}] to cloud pixel speed in [pixel s^{-1}] from a single sky imager. The combination of a cloud speed sensor and sky imager makes measurements of CBH more affordable and convenient compared to a ceilometer. Ceilometers cost about $20k while the bill of material for the CSS is less than $400. Further a CSS could be directly integrated into the enclosure of a sky imager avoiding the need for separate setup site and power and Ethernet connectivity.

16 days are analyzed with the proposed method. Overall, the method shows promising results with average nRMSD of 17.4% compared against on-site ceilometer measurements. The CBH accuracy depends on the accuracy of CSS cloud speed and the USI cloud pixel speed. Also, multiple layers of cloud with different direction and/or speed could degrade the performance because both CSS and USI are only able to determine cloud speed of one single cloud layer. Future efforts will focus on improving both CSS and USI cloud speed algorithms.

A ramp rate control algorithm for BESS and inverter control to mitigate ramp rates in power output from a PV system was developed. The control algorithm uses image-based solar forecasts to predict future fluctuations in PV power output ("ramps") and schedules optimal control of a BESS and inverter—the BESS provides and absorbs power in concert with fluctuating power output from the PV system to mitigate up- and down-ramps; the inverter curtails energy by adjusting the efficiency of the PV system to mitigate up-ramps. Inputs to the ramp rate control

algorithm are almost entirely internal to the PV-BESS-inverter-forecast system; the maximum permissible ramp rate is the only outside input.

Requirements for ramp rate mitigation from PV systems will likely increase in the future with high PV penetration, and operators of PV arrays without BESS or other storage installed behind-the-meter will have to consider installing such systems. Ultimately, economics—between the monetization of ramp violations, BESS capital cost, BESS lifetime, and the value of PV power generation via market rates, purchase agreements, or feed-in tariffs—will drive BESS investment decisions, including the choice of BESS capacity. Though such monetizations are outside the scope of this work, an exploration of BESS sizing on ramp rate mitigation provides initial insight into the optimal BESS sizing in a future where monetizations exist.

Larger BESS capacities improve ramp violation mitigation, but with diminishing returns. Increasing the BESS dispatch capacity from 1-4 kW increases mitigation most rapidly; mitigation improves thereafter but at a decreasing rate. Increasing the BESS energy capacity from 0.083-0.25 kWh also increases mitigation. A BESS with a given energy capacity reaches a point where increases in the dispatch capacity do not improve mitigation. The same is true for a given dispatch capacity and increasing energy capacities. These trends in BESS sizing versus mitigation show that both capacities must be increased proportionally to one another to achieve effective ramp violation mitigation.

The best-case improvement in BESS dispatch and inverter control is observed when using perfect forecasts—that is, when perfect information about upcoming ramps is available. Such a method is in practice impossible but nevertheless provides an upper limit to the utility forecasting can provide with a given ramp rate control algorithm. Because short-term solar forecasting is non-trivial, and errors do occur, the results of ramp rate control in separate sets of simulations—first using perfect forecasts and second persistence forecasts (which is equivalent to no forecast methodology)—provide bounds of sorts on the results of simulations with sky imager forecasts. Sufficiently accurate sky imager forecasts will provide better ramp mitigation than persistence forecasts, but will not beat perfect forecasts. Two questions then arise: one, to what degree and in what situations do sky imager forecasts outperform persistence forecasts; and two, are additional costs incurred to achieve such outperformance?
With regard to the first question, in general the sky imager forecasts are superior; however, the combination of many cloudy days, forecast errors, and a small BESS dispatch capacity can reduce mitigation potential. In these cases, the persistence forecasts are superior. The answer to the second question is clear: to outperform persistence forecasts, the sky imager forecasts require greater BESS cycling and inverter curtailment due to forecast error.

10. Ratepayer Benefits

The variable nature of solar power is of concern to electric grid operators in California where dramatic growth in PV installations is occurring. As already experienced in Puerto Rico, Hawaii and other island grids, if short term solar variability cannot be predicted or reduced, the integration cost of solar power increases through investment in large local energy storage

systems or regulation capacity by the grid operator. Although some of the short-term variability is reduced through geographic diversity, the residual effect is significant in high PV penetration areas. At the microgrid and distribution feeder level, the geographic diversity is less available, causing voltage issues affecting service quality and reliability.

Independent of energy storage emerging as an economically viable technology, regulatory action imposed requirements for the California IOU's to procure energy storage. In this case, forecast and control systems such as the one proposed here will be needed to operate these systems in a way to benefit solar power integration. CPUC rulemaking 10-12-007 "Decision Adopting Energy Storage Procurement Framework and Design Program" envisions 1,325 MW of IOU energy storage by 2020 with the first deployments as early as 2014. The time is ripe to design control systems that enable higher solar penetration.

The work will also increase the capacity value of distributed solar PV in microgrids. Temporary cloud cover can substantially reduce solar production and result in peak net demand to the grid with associated demand charges. The algorithm will reduce demand charges by ensuring batteries are fully charged before sudden drops in PV output. While the robustness of the algorithm needs to be improved before it will successfully reduce monthly demand charges, which requires high reliability, similar applications exist for autonomous operations of microgrids in case of a power outage.

A more important benefit would be reductions in voltage fluctuations for microgrids by avoiding rapid power changes and/or ensuring that the ramping capacity of any backup power supply such as diesel generators is not exceeded during cloud transients.

This integrated system of short-term solar forecasting using sky imagery, control algorithms, and relatively small energy storage systems presents a unique synthesis of technologies with high potential in firming solar generation.

This project uses technology that is being applied in a CSI RD&D Solicitation #3 research project to conduct short-term forecasting and distribution feeder power flow modeling and control. The forecast accuracy of these sky imaging systems was limited by unknown cloud height. Furthermore, control algorithms were not advanced and hardware was not available to demonstrate the functionality. This project leverages prior work to improve the accuracy of the solar forecasts and conduct real demonstrations with advanced control algorithms.